



ISSN 0975-413X
CODEN (USA): PCHHAX

Der Pharma Chemica, 2016, 8(19):155-165
(<http://derpharmachemica.com/archive.html>)

Essential Oil of *Brachychiton* as Eco-Friendly Green Inhibitor for the Corrosion Control of Mild steel in Hydrochloric Acid Medium

A. Aitlaalim¹, M. Boudalia², F. Ouanji¹, S. Echihi^{2,3}, A. Guenbour²,
A. Belleaouchou², M. Tabyaoui², M. Kacimi¹ and A. Zarrouk⁴

¹Laboratory of Materials, Catalysis and Environment (CNRST-URAC 26), University of Mohammed V, Faculty of Sciences, Rabat, Morocco

²Laboratory of Nanomaterials, Nanotechnology and Environment, Faculty of Science, University of Mohamed-V- Av. IbnBattouta, BP 1014 Agdal-Rabat, Morocco

³Laboratory of Water and Environment, Faculty of Sciences of Chouaib doukkali, BP 20, 24000 El jadida, Morocco

⁴LC2AME-URAC 18, Faculty of Science, First Mohammed University, PO Box 717, 60 000 Oujda, Morocco

ABSTRACT

Corrosion inhibition of mild steel in normal hydrochloric acid solution at 303 K by *Brachychiton* essential oil (B.O.) has been studied by potentiodynamic polarization and Electrochemical Impedance Spectroscopy (EIS) measurements. The oil essential of *Brachychiton* (B.O.), was analyzed by chromatography (HPLC/UV) and FTIR spectra. The results show that this oil is characterized by palmitoleic acid, palmitic acid, stearic acid, oleic acid being the major constituents. The inhibition efficiency increases with the increase of inhibitor concentration. Potentiodynamic polarization studies clearly reveal that the presence of this inhibitor acts like a mixed inhibitor. The effect of temperature on the corrosion behavior of mild steel in 1M HCl with and without oil in the temperature range 303-333 K, indicates that inhibition efficiency increases with temperature. While SEM analysis the formation of protective layer over the steel surface. The adsorption of natural product on the mild steel surface obeys to Langmuir's adsorption isotherm.

Keywords: Mild steel, Corrosion inhibition, *Brachychiton* plant, Electrochemical techniques, HPLC/UV, FTIR spectra.

INTRODUCTION

Corrosion is a phenomenon where chemistry helps to explain its mechanism. It is simply a destruction of materials resulting from an exposure and the interaction with the environment. Corrosion can be defined as the environmentally induced degradation of a material that involves a chemical reaction [1].

Degradation implies deterioration of physical properties of the material. This can be a weakening of the material due to a loss of cross-sectional area, the shattering of a metal due to hydrogen embrittlement, or the cracking of a polymer due to sunlight exposure [2]. Corrosion of a metal is due to chemical or electrochemical reactions when it comes in contact with matters present in its environment. However, corrosion can be controlled by the metal is in contact the environment which stifles the anodic or cathodic reaction or both, and this is achieved by the use of inhibitors [3]. Each metal is subjected to its own unique corrosion process. Mild steel has been extensively used under different conditions in chemical and allied industries in handling alkaline, acid and salt solution. The corrosion of metals in acid solutions can be inhibited by a wide range of substances, which may be synthetic or natural inhibitors. Synthetic compounds containing multiple bonds and hetero atoms are effective inhibitors [4-13], but at the same time the processing time, their cost and their toxic nature have compelled the researchers to look for eco-friendly, nontoxic and low cost inhibitors for the corrosion protection of metals. One of the latest and popular

approaches is the use of environmental non-toxic inhibitor. In view of this, many alternative eco-friendly corrosion inhibitors have now been developed, *Ginger* [14], *henna* [15], *thym* [16], *jojoba oil* [17], *Phaseolus vulgaris L.* [18], *Acacia Trees* [19], *Xylopia Ferruginea* [20], *Bauhinia purpurea leaves* [21], *Hibiscus cannabinus* [22], *Black Pepper* [23]. The extract of this plant have been successfully used for the prevention of steel corrosion in HCl, H₃PO₄ and H₂SO₄, and it has been found very effective [2,19,20].

The *Brachychiton* is a genus of 31 species of trees and large shrubs, native to Australia for 30 of them, and to New Guinea for 1 of them. It is sometimes called as a “bottle tree” because of the shape of its trunks. It is a genus, according to the conventional classification, of the Sterculiaceae family. According to the phylogenetic classification, the genus is included in the Malvaceae family. The latter is represented in the spontaneous state in the Moroccan flora by ten genera [24]. In Morocco, the *Brachychiton* genus exists only in the ornamental state, following its introduction as an alignment plant. These trees are rarely shrubs with smooth bottle-shaped trunk; hence their name of ‘bottle trees’ [25].

As a contribution to the current interest on eco-friendly corrosion inhibitors, the present work is devoted to study the effect of one of the fruits of trees which in our case the *brachychiton*, existing in Moroccan parks, our work is essentially devoted to investigate the effect of *Brachychiton* essential oil (B.O.) as corrosion inhibition for mild steel in HCl solution using potentiodynamic polarization measurements and electrochemical impedance spectroscopy (EIS). The thermodynamic parameters for activation processes were calculated and discussed.

MATERIALS AND METHODS

Preparing sample and essential oil extraction

The ground seeds (5 g) and a volume of n-hexane (seed-to-solvent ratio of 1:6.5 mL/g) were added to an Erlenmeyer flask (100 mL), connected to a condenser. The flask was placed in a thermostated water bath at a predetermined temperature (45°C). No mixing was applied. At the end of a predetermined extraction time, the liquid extract was separated from the exhausted seeds by vacuum filtration. The cake was then washed twice with n-hexane (20 mL). The combined filtrates were evaporated to a constant mass at 50°C under vacuum. The sample oil yield was defined as the amount of the oil extracted from 100 g of seeds. Each experiment was carried out in duplicate.

Analysis Chromatography by HPLC / UV

The identification of the components of vegetable oils is usually done by various types of chromatography, but the analysis of the profiles of triglycerides (TAGs) is best studied by HPLC. [26] It has been reported that UV detection at short wavelength (205 or 210 nm) provided a linear answer with a mean sensitivity [27-29]. By against the use of the refractive index as a mean of detection, cannot be applied with elution in [28] gradient mode. On the other hand, the HPLC / MS coupling method provides linear responses with excellent sensitivity [28,30,31]. M.J. Lerna-Garcia and Coll. developed HPLC / UV method for the prediction of the botanical origin of the various vegetable oils. [32] In this study, identifying 26 TAGs has been reported using a colonne Kintex C18 100A (150 mm × 4.6 mm, 2.6 micro) Phenomenex brand. The mobile phase consists of 30% n-pentanol and 70% acetonitrile. Note that the identification by HPLC involves comparing the retention time of the peaks of standard relative to those of the sample with a tolerance of ± 5%.

In our case the identification of TAGs present in our extract is difficult given the lack of standards. Therefore we have to compare HPLC profiles obtained by the extraction method. For this we adopted the protocol described above with a few modifications in the composition of the mobile phase and the column used.

The separation method was applied to samples of vegetable oil. The chromatogram of the *brachychiton* oil is shown in Figure 1. 17 peaks in total were identified within 10 min analysis.

The identification of tags according to the protocol described below has led us to determine areas of abundance of a common acid between the identified triglycerides. The area between 3-6 min finds TAGs using a fraction of the acid linoleic (LLLn: dilinolein-linolenic acid, LLL: trilinolein acid, OLLn: oleic-linoleic-linolenic acid, OLL: oleic-linoleic acid, LLP: dilinolein-palmitic acid). In the next zone between 6-8min located in the fraction predominant in TAGs present and that of oleic acid (OOO: triolein acid, OOP: diolein -palmitic acid). The area between 7-9 min, the palmitic takes fraction below (PPO: dipalmitic-oleic acid, PPP: tripalmitic acid). With the presence of TAGs with an upper bound fraction of stearic acid (SSL: stearic di-linolein acid) to 9.5min and also that of gadoleic acid (GLL: gadoleic-dilinolein acid) to 4 min.

Figure 1: HPLC-UV chromatogram oil Brachychiton

FTIR spectroscopy analysis

The experimental technique used frequently to characterize the vibration of functional groups is the IR spectroscopy. The spectrum was recorded in ATR from pure oil samples.

The FTIR spectrum of the recorded sample at room temperature is shown in figure 2.

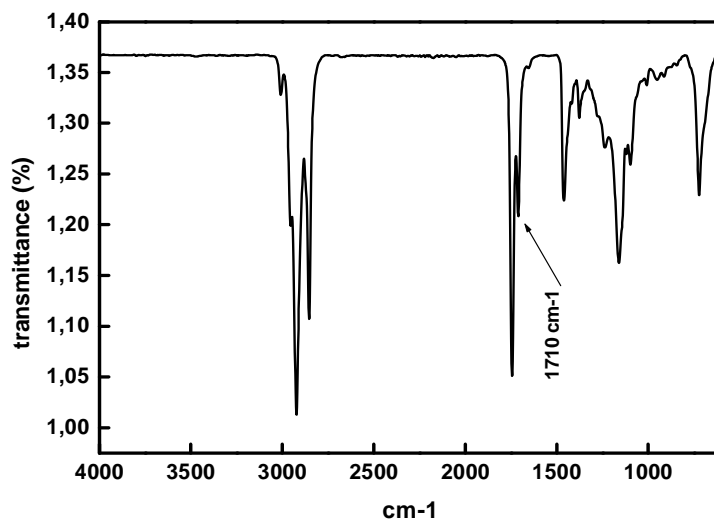


Figure 2: FTIR spectra of the samples studied

In general, we note that the pace of the IR spectrum shows similarity with those of vegetable oils [33-36].

Note that the functions of the bands corresponding to the stretching vibration modes are usually easier than the corresponding bands to bending vibration modes. This is mainly due to overlap for one and / or more bands.

The spectrum of the studied sample shows that more bands are common regardless of the extraction mode. The vibrations of the C-H groups can be observed in the region 3000-2800 cm⁻¹. In effect, two distinct bands are visible at approximately 2923 and 2853cm⁻¹ which respectively correspond to symmetric and asymmetric elongations of the -CH₂ groups. The absorptions at 2953 cm⁻¹ and the shoulder to 2872 cm⁻¹ are characteristics for symmetrical and

asymmetrical movements $-\text{CH}_3$ moieties. The vibrations of deformations of these groups (CH_2 and CH_3) appear respectively in 1461, 1377 and 722 cm^{-1} .

The position of the band relative to the elongation movement carbonyl groups ($\text{C}=\text{O}$) appears green 1744 cm^{-1} . Symmetrical and asymmetrical deformations of these groups appear around 1100 and 1120 cm^{-1} . Bitter literature, band to 1161 cm^{-1} is attributed to the C-O vibration associated with a ester moiety [36]. The strong band at about 1710 cm^{-1} corresponds to the vibration of the free carboxylic acid groups.

MATERIALS

The Mild steel was used for this study has the following composition: it contains 0.09 % P; 0.38 % Si; 0.01 % Al; 0.05 % Mn; 0.21 % C; 0.05 % S and the remainder iron.

The specimen was used for electrochemical measurements. The exposed surface area was 1 cm^2 . The surface preparation was carried out with emery papers by increasing grades (400, 600 and 1200 grit size), then degreased with AR grade ethanol and dried at room temperature before use. The aggressive solutions of 1M HCl was prepared by dilution of analytical grade 37% HCl with double distilled water.

Electrochemical tests

Electrochemical impedance spectroscopy

The electrochemical measurements were carried out using Volta lab (Tacussel- Radiometer PGZ 301) potentiostat and controlled by Tacussel corrosion analysis software model (Volta master 4) at under static condition. The Studies were done by using conventional three electrode Pyrex glass cell with platinum as counter electrode and SCE as reference electrode. The working electrode was a mild steel electrode. All potentials given in this study were referred to this reference electrode. The working electrode was immersed in test solution for 0.5 hours to establish steady state open circuit potential (E_{ocp}). After measuring the E_{ocp} , the electrochemical measurements were performed. All electrochemical tests have been performed in aerated solutions at 303 K. The EIS experiments were conducted in the frequency range with high limit of 100 KHz and different low limit 10 m Hz at open circuit potential, by applying 10 mV ac voltage peak-to-peak. The R_p and C_{dl} values were obtained from the Nyquist plots. The η was calculated as:

$$\eta_z \% = \frac{R_p^i - R_p^\circ}{R_p^i} \times 100 \quad (1)$$

Where, R_p° and R_p^i are the polarization resistance in absence and in presence of inhibitor, respectively.

All the experiments are repeated three times to ensure the reproducibility

Potentiodynamic polarization

The electrochemical behavior of mild steel sample in inhibited and uninhibited solution was studied by recording anodic and cathodic potentiodynamic polarization curves. Measurements were performed in the 1.0 M HCl solution containing different concentrations of the tested inhibitor by changing the electrode potential automatically from -800 to 0 mV versus corrosion potential at a scan rate of 1 mV/s. The electrochemical parameters such as corrosion current density (I_{corr}), corrosion potential (E_{corr}), anodic and cathodic slopes (β_a and β_c) were obtained from Tafel plots and the η was determined using the formula as follows:

$$\eta_{\text{Tafel}}(\%) = \frac{I_{\text{corr}} - I_{\text{corr}(i)}}{I_{\text{corr}}} \times 100 \quad (2)$$

where I_{corr} and $I_{\text{corr}(i)}$ are the corrosion current densities for steel electrode in the uninhibited and inhibited solutions, respectively.

Surface analysis

The test coupons of the size 1 $\text{cm} \times 1 \text{cm} \times 0.1 \text{cm}$ were exposed in 1 M HCl solutions in absence and presence of 1.2 g/L of the (B.O.) for 6 hours at 298 K and then washed with distilled water. After elapsed time mild steel specimens were taken out and cleaned with double distilled water, dried with cold air blower and finally the scanning electron microscopy micrographs were recorded using SEM model Quanta 200 FEI Scanning instrument at an accelerating voltage of 20kV at 2000 \times magnification.

RESULTS AND DISCUSSION

Potentiodynamic Polarization Curves

Effect of concentration

The potentiodynamic polarization data are shown in Figure 3 as the Tafel plots for mild steel in 1M HCl solution with the addition of various concentrations of the additive of *Brachychiton oil* (B.O.). The corrosion kinetic parameters such as E_{corr} , I_{corr} , anodic and cathodic Tafel slopes were derived from these curves and are given in Table 1. The values of η % were calculated using the eq (2).

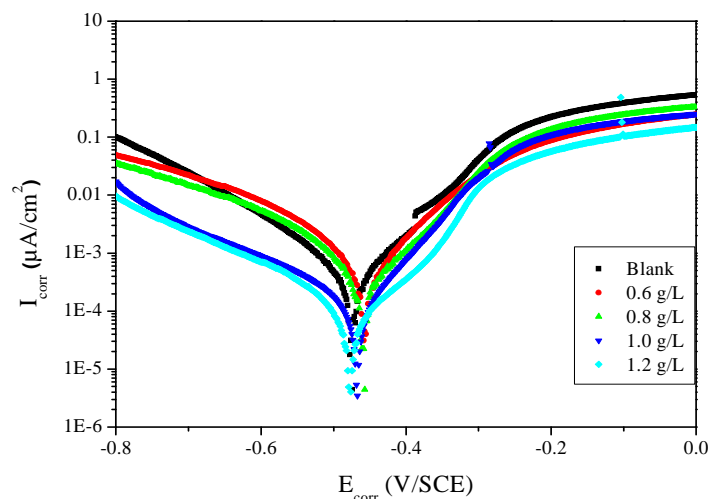


Figure 3: Potentiodynamic polarization curves of mild steel in 1M HCl in the presence of different concentrations of (B.O.) at 303 K

Table 1: Electrochemical parameters of mild steel in 1M HCl solution without and with (B.O.) at different concentrations

Medium	Conc (g/L)	$-E_{\text{corr}}$ (mV/SCE)	I_{corr} ($\mu\text{A}/\text{cm}^2$)	$-\beta_c$ (mV/dec)	β_a (mV/dec)	η_{Tafel} (%)	θ
HCl	—	441	579	138.0	135.0	—	—
(B.O.)	1.2	478	47	88.3	97.9	91.0	0.910
	1.0	465	59	102.1	71.5	89.8	0.898
	0.8	456	70	71.7	85.3	87.9	0.879
	0.6	454	83	77.4	78.2	85.6	0.856

We remark that the cathodic current-potential curves give rise to parallel Tafel lines, which indicate that hydrogen evolution reaction is activation controlled and that the addition of the (B.O.) does not modify the mechanism of this process (Figure 3) [37]. As it is shown in Table 1, (B.O.) inhibit the corrosion process and the inhibition efficiency values (η) increases with the concentration of inhibitor, reaching its maximum value to attain 91% at 1.2 g/L. These data show that the increase in inhibitor concentration leads to decrease in the corrosion current density. The addition of *Brachychiton essential oil* (B.O.) causes a shift in the values of E_{corr} slightly toward anodic value (more negative) compared to the blank but no definite shift in E_{corr} is detected. The magnitude of change in the E_{corr} values (less than 85 mV) indicate that (B.O.) acts as mixed type inhibitor [38] with predominantly cathodic effect, i.e., cathodic evolution of hydrogen gas is more favored than the anodic dissolution of steel. Both β_a and β_c were affected; this was indicative of the mixed-mode inhibitive nature of the inhibitor.

Effect of temperature

The effect of temperature on the inhibition performance of (B.O.) for mild steel in 1M HCl solution in the absence and presence of 1.2 g/L concentration at temperature ranging from 303 to 333 K was obtained by potentiodynamic polarization measurements. The results are given in Table 2. The inhibition efficiencies are found to decrease with increasing the solution temperature from 303 K to 333 K. This behavior can be interpreted on the basis that the increase in temperature results in desorption of the inhibitor molecules from the surface of mild steel. Table 2 shows that the corrosion rate increased with increasing temperature both in uninhibited and inhibited solutions. The corrosion rate increases more rapidly with temperature in the absence of the inhibitor.

Table 2: Effect of temperature on the corrosion rate of mild steel at 1.2 g/L of (B.O.) at different temperatures

Temperature (K)	I_{corr} ($\mu\text{A}/\text{cm}^2$)		η_{Tafel} (%)
	Blank	(B.O.)	
303	579	47	91
313	692	100	85
323	1644	250	84
333	2102	378	82

A plot of the logarithm of the corrosion rate ($\mu\text{A cm}^{-2}$) of carbon steel obtained from potentiodynamic polarization vs. $1000/T$ gave a straight line as shown in Fig.4. The apparent activation energy (E_a) was calculated by using following Arrhenius equation:

$$\ln(I_{corr}) = \ln A - \frac{E_a}{RT} \quad (3)$$

where E_a is the apparent activation corrosion energy, T is the absolute temperature, A is the Arrhenius pre-exponential constant and R is the universal gas constant.

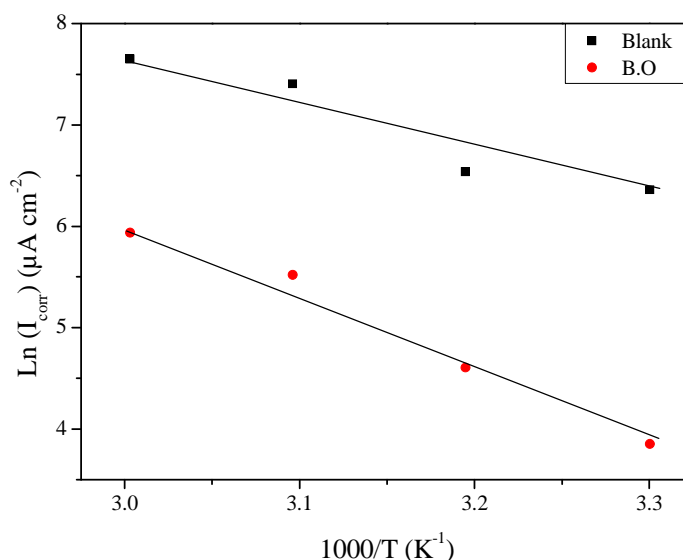


Figure 4: Arrhenius plots of steel in acid with and without 1.2 g/l (B.O.) in 1M HCl

An alternative formulation of Arrhenius equation is [39]:

$$I_{corr} = \frac{RT}{Nh} \exp\left(\frac{\Delta S_a}{R}\right) \exp\left(\frac{\Delta H_a}{RT}\right) \quad (4)$$

where h is Planck's constant, N is Avagadro's number, ΔS_a is the entropy of activation and ΔH_a is the enthalpy of activation. Figure 5 shows a plot of $\ln(I_{corr}/T)$ vs. $1/T$.

The values of E_a , ΔH_a and ΔS_a were estimated from the slopes of the straight lines and given in Table 3.

The value of E_a found for (B.O.) is higher than that obtained for 1M HCl solution. The increase in the apparent activation energy may be interpreted as physical adsorption [40,41].

Straight lines are obtained with a slope of $\frac{\Delta H_a}{R}$ and an intercept of $\ln R/Nh + \frac{\Delta S_a}{R}$ from which the values of

ΔS_a and ΔH_a are calculated and are given in Table 3.

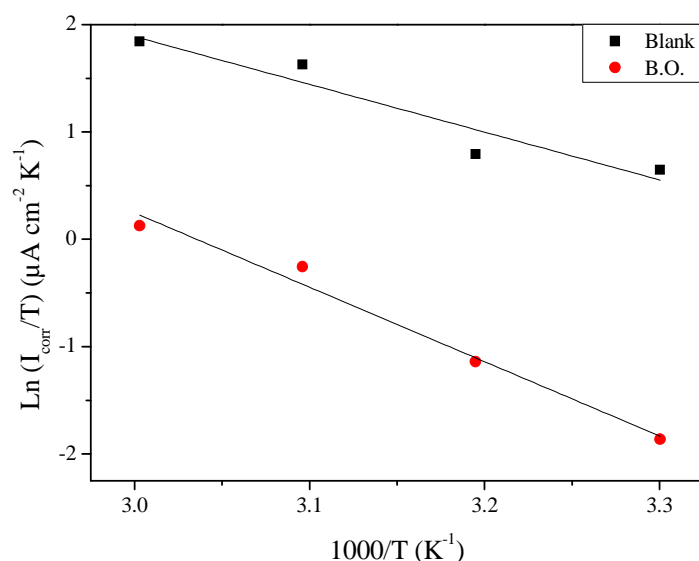


Figure 5: Transition Arrhenius plots of $\text{Ln}(I_{\text{corr}}/T)$ vs. $1/T$ for steel in 1M HCl in the absence and the presence of (B.O.) at optimum concentration

Table 3: Activation parameters for the steel dissolution in 1M HCl in the absence and the presence of (B.O.) at optimum concentration

Medium	Linear regression coefficient (r)	E_a (kJ/mol)	ΔH_a (kJ mol ⁻¹)	ΔS_a (J K ⁻¹ mol ⁻¹)
Blank	0.99742	39.6	36.9	-69.3
(B.O.)	0.99663	60.3	57.6	-169.6

The positive sign of ΔH_a reflect the endothermic nature of the steel dissolution process suggesting that the dissolution of steel is slow in the presence of inhibitor [42] whereas large negative values of entropies ΔS_a imply that the activated complex in the rate determining step represents an association rather than a dissociation step, meaning that a decrease in disordering takes place on going from reactants to the activated complex [42]. From the previous data, we can say that (B.O.) essential oil can be used as an effective inhibitor.

Adsorption isotherm

Basic information on the interaction between the inhibitor and mild steel surface are investigated by the adsorption isotherms. For this purpose, the values of surface coverage (θ) at different concentrations of (B.O.) in acid media at 303 K have been used to explain the best isotherm to determine the adsorption process. The value of the surface coverage (θ) was calculated using the relationship [43]:

$$\theta = \frac{\eta_{\text{Tafel}}(\%)}{100} \quad (5)$$

Attempts were made to fit these θ values to various isotherm including Langmuir, Temkin, Frumkin, Freundlich, etc. The best fit was obtained with Langmuir isotherm as suggested by the plot between C/θ and C (as shown in figure 6) and the linear correlation coefficient of the fitted data was close to 1, indicating that the adsorption of the inhibitor molecules obey the Langmuir's adsorption isotherm as expressed as:

$$\frac{\theta}{1-\theta} = C K_{\text{ads}} \quad (6)$$

Where C is the inhibitor concentration and K_{ads} is the equilibrium constant for adsorption/desorption process of the inhibitor molecules on the metal surface. K_{ads} values were calculated from the intercept of the plot for adsorption process. The adsorption equilibrium constant, K_{ads} , is related to the standard free energy ($\Delta G_{\text{ads}}^\circ$) by the following equation:

$$\Delta G_{ads}^{\circ} = -RT \ln(C_{H_2O} K_{ads}) \quad (7)$$

where the $C_{H_2O} = 1000$ g/L in the solution.

For the determination of absorption nature, it is difficult to distinguish between chemisorption and physisorption only based on these criteria, especially when charged species are adsorbed. The possibility of Coulomb interactions between adsorbed cations and specifically adsorbed anions can increase the Gibbs energy even if no chemical bond appears [44]. However, the calculation of the ΔG_{ads}° value of (B.O.) is not possible because the molecular mass of the extract components is not known. This limitation is noted by some authors in the case of the essential oils used as corrosion inhibitors for steel in acidic media [45,46].

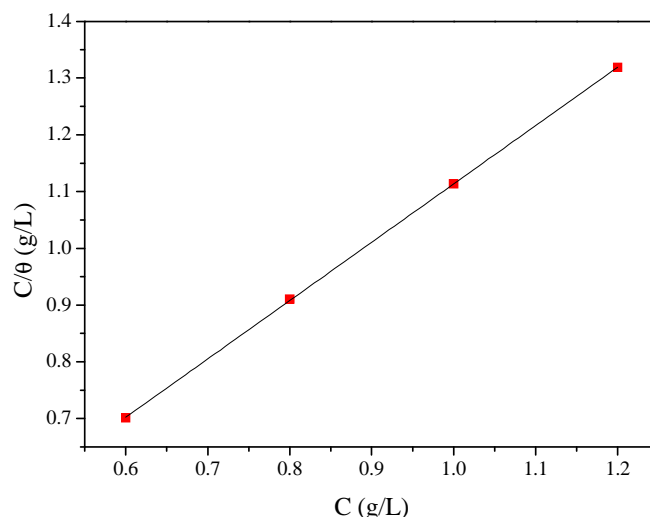


Figure 6: Langmuir adsorption isotherm for mild steel in 1M HCl solution of B.O. at different concentrations

Electrochemical impedance spectroscopy

EIS technique was applied to investigate the electrode/electrolyte interface and corrosion processes that occur on mild steel surface in presence and absence of (B.O.) To ensure complete characterization of the interface and surface processes, EIS measurements was made at OCP in a wide frequency range at 303 K. Figure 7 shows Nyquist plots for mild steel electrode immersed in 1M HCl solution at 303 K in absence and presence of various concentrations of the essential oil. It is clear from the figure 7 that the diameter of the semicircle increases with the increase in concentration of the (B.O.) inhibitor, indicating an increase in corrosion resistance of the metal.

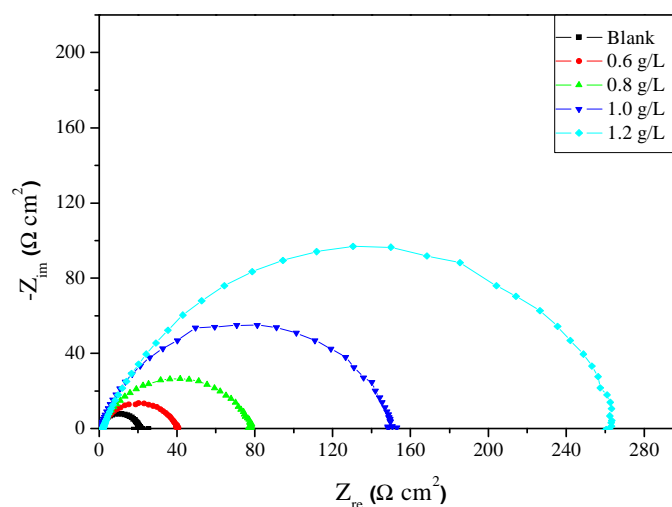


Figure 7: Nyquist plots for mild steel in 1M HCl containing different concentrations of (B.O.)

The value of electrochemical double layer capacitance (C_{dl}) was calculated at the frequency, f_{max} using the following equation [4]:

$$C_{dl} = \frac{1}{2\pi f_{max} R_p} \quad (8)$$

with C_{dl} Double layer capacitance ($\mu\text{F cm}^{-2}$); f_{max} : maximum Frequency (Hz) and R_p : Polarization resistance ($\Omega \text{ cm}^2$).

The impedance data listed in the table 4 indicate that the values of both R_p and $\eta_z\%$ are found to increase with increase in concentration of the extract, while the values of C_{dl} are found to decrease. This behavior can be attributed to a decrease in dielectric constant and/or an increase in thickness of the electric double layer, suggesting that the essential oil molecules act by adsorption mechanism at mild steel/acid interface [47].

Table 4: AC impedance data of mild steel in 1M HCl acid solution containing different concentrations of (B.O.) at 303 K

Medium	Conc (g/L)	R_p ($\Omega \text{ cm}^2$)	C_{dl} ($\mu\text{F/cm}^2$)	f_{max} (Hz)	η_z (%)
HCl	—	20	200	40.0	—
B.O.	1.2	262	48.6	12.5	92.3
	1.0	155	51.3	20.0	87.0
	0.8	88	57.2	31.6	77.0
	0.6	50	79.6	40.0	60.0

A low capacitance may result if water molecules at the electrode interface are largely replaced by organic inhibitor molecules through adsorption [48]. The larger inhibitor molecules also reduce the capacitance through the increase in the double layer thickness [49]. The inhibiting effectiveness increases with the concentration of the inhibitor to reach a maximum value from 92.3% for (B.O.).

Surface analysis by SEM

The surface morphology of mild steel was studied by scanning electron microscopy, the figure 8 shows an SEM photograph recorded for mild steel samples Polished (a) and exposed for 6 h in 1M HCl solution without (B.O.) (b) and with 1.2g/L of *Brachychiton Oil* at 303 K .

It can be seen from Fig. 8a that the mild steel sample before immersion seems smooth and shows some abrading scratches on the surface. Inspection of Fig. 8b reveals that the mild steel surface after immersion in uninhibited 1M HCl shows an aggressive attack of the corroding medium on the steel surface. The morphology in Fig. 8c shows a rough surface, that corrosion does not occur in presence of inhibitor and hence corrosion was inhibited strongly when the inhibitor was present in the hydrochloric, and the surface layer is very rough. In contrast, in the presence of 1.2 g/L *Brachychiton Oil*, the steel surface was corroded only negligibly, which further confirm the inhibition action. In addition, there is an adsorbed film on mild steel surface (Fig. 8c).

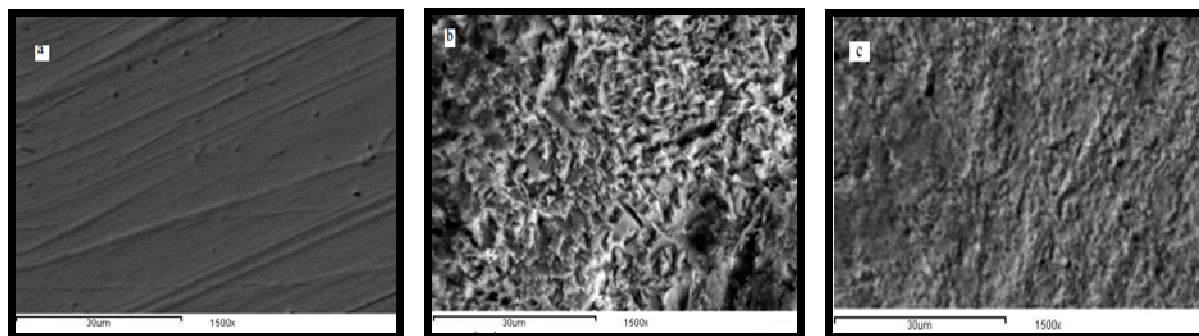


Figure 8: SEM micrographs of mild steel surface: (a) before of immersion in 1M HCl, (b) after 6h of immersion in 1M HCl and (c) after 6 h of immersion in 1M HCl + 1.2g/L of (B.O.) at 303 K

CONCLUSION

From the overall studies the following conclusions could be deduced:

Brachychiton Oil examined acted as an efficient corrosion inhibitor in 1M HCl. Polarization studies showed that oil was a mixed inhibitor and its inhibition efficiency increased with the inhibitor concentration but decreases with the increase of temperature. Impedance method indicates that oil adsorbs on the mild steel surface with increasing transfer resistance and decreasing of the double-layer capacitance. The adsorption of (B.O.) on the mild steel surface follows the Langmuir adsorption isotherm. The inhibitor efficiency determined by electrochemical methods and methods potentiodynamic curves are in good agreement.

REFERENCES

- [1] D.J. Duquette, R.E. Schafrik, D.C. Washington: National Academy of Sciences, **2011**.
- [2] M. Boudalia, A. Guenbour, A. Bellaouchou, A. Laqhaili, M. Mousaddak, A. Hakiki, B. Hammouti, E.E. Ebenso, *Int. J. Electrochem. Sci.* **2013**, 8, 7414.
- [3] B. Sanyal, *J. Chem. Acta*, **1981**, 9, 165.
- [4] H. Zarrok, H. Oudda, A. El Midaoui, A. Zarrouk, B. Hammouti, M. Ebn Touhami, A. Attayibat, S. Radi, R. Touzani, *Res. Chem. Intermed.* **2012**, 38, 2051.
- [5] A. Zarrouk, B. Hammouti, H. Zarrok, M. Bouachrine, K.F. Khaled, S.S. Al-Deyab, *Int. J. Electrochem. Sci.* **2012**, 6, 89.
- [6] A. Zarrouk, B. Hammouti, A. Dafali, H. Zarrok, *Der Pharm. Chem.* **2011**, 3 (4), 266.
- [7] H. Zarrok, A. Zarrouk, R. Salghi, H. Oudda, B. Hammouti, M. Assouag, M. Taleb, M. Ebn Touhami, M. Bouachrine, S. Boukhris, *J. Chem. Pharm. Res.* **2012**, 4, 5056.
- [8] A. Ghazoui, A. Zarrouk, N. Bencat, R. Salghi, M. Assouag, M. El Hezzat, A. Guenbour, B. Hammouti, *J. Chem. Pharm. Res.* **2014**, 6, 704.
- [9] H. Zarrok, A. Zarrouk, R. Salghi, M. Assouag, B. Hammouti, H. Oudda, S. Boukhris, S.S. Al Deyab, I. Warad, *Der Pharm. Lett.* **2013**, 5, 43.
- [10] M. Belayachi, H. Serrar, H. Zarrok, A. El Assyry, A. Zarrouk, H. Oudda, S. Boukhris, B. Hammouti, E. Ebenso Eno, A. Geunbour, *Int. J. Electrochem. Sci.* **2015**, 10, 3010.
- [11] A. Zarrouk, H. Zarrok, R. Salghi, R. Touir, B. Hammouti, N. Benchat, L.L. Afrine, H. Hannache, M. El Hezzat, M. Bouachrine, *J. Chem. Pharm. Res.* **2013**, 5, 1482.
- [12] H. Zarrok, A. Zarrouk, R. Salghi, M. Ebn Touhami, H. Oudda, B. Hammouti, R. Touir, F. Bentiss, S.S. Al-Deyab, *Int. J. Electrochem. Sci.* **2013**, 8, 6014.
- [13] D. Ben Hmamou, M.R. Aouad, R. Salghi, A. Zarrouk, M. Assouag, O. Benali, M. Messali, H. Zarrok, B. Hammouti, *J. Chem. Pharm. Res.* **2012**, 4, 3498.
- [14] E. Chaieb, A. Bouyanzer, B. Hammouti, M. Ben kaddour, *Appl. Surf. Sci.* **2005**, 246, 199.
- [15] B. Hammouti, S. Kertit, M. Melhaoui, *Bull. Electrochem.* **1995**, 11, 553.
- [16] B. Hammouti, S. Kertit, M. Melhaoui, *Bull. Electrochem.* **1997**, 13, 97.
- [17] A. Bouyanzer, B. Hammouti, *Resin Technol.* **2004**, 33, 287.
- [18] A.M. Abdel-Gaber, B.A. Abd-El-Nabey, I.M. Sidahmed, A.M. El-Zayady, M. Saadawy *Corros. Sci.* **2006**, 48, 2765.
- [19] A. Bouyanzer, B. Hammouti, L. Majidi, B. Haloui, *Port. Electrochim. Acta*, **2010**, 28, 165
- [20] W.A.W. Elyn Amira, A.A. Rahim, H. Osman, K. Awang, P. Bothi Raja, *Int. J. Electrochem. Sci.* **2011**, 6, 2998.
- [21] N. S. Patel, S. Jauhari, G. N. Mehta, *Arab. J. Sci. Eng.* **2009**, 34, 6.
- [22] M.R. Singh, G. Singh, *J. Mater. Environ. Sci.* **2012**, 3, 698.
- [23] M.A. Quraishi, D.K. Yadav, I. Ahamad, *TOCORR*, **2009**, 2, 56.
- [24] M. Fennane, M. IbnTattou. Travaux de l'Institut Scientifique, Série Botanique **2005**, 37, 487.
- [25] AGFACTS, 647. Dept Ag. NSW.
- [26] R. Aparicio-Ruiz, *J. Chromatog A*, **2000**, 881, 93.
- [27] M. Holcapek, M. Lisa, P. Jandera, N. Kabatova, *J. Chromatog. A*, **2005**, 1087, 112.
- [28] M. Lisa, M. Holcapek, *J. Chromatog. A*, **2008**, 1198, 115
- [29] M. Holcapek, P. Jandera, *J. Chromatog. A*, **2001**, 926, 175.
- [30] K.Nagy, D.Bongiorno, G.Avellone, P.Agozzino, L.Ceraulo, K.Vekey, *J. Chromatog. A*, **2005**, 90, 1078.
- [31] M. Lisa, M. Holcapek, M. Bohac, *J. Chromatog. A*, **1999**, 858, 13.
- [32] M.J. Lerma-García, R. Lusardi, E. Chiavaro, L. Cerretani, A. Bendini, G. Ramis Ramos, E.F. Simó-Alfonso, *J. Chromatog. A*, **2011**, 1218, 7521.
- [33] M. Safar, D. Bertrand, M.F. De value, C.Genet, *JAOC*, **1994**, 71, 4.
- [34] M.D. Guille, N. Cabo, *J. Sci. Food. Agric.* **1997**, 75, 111.
- [35] A. Rohmana, Y.B. Che Man, *Vib. Spectrosc.* **2011**, 55, 141.
- [36] Q. Ren, T. Zhao, *Carbohydr. Polym.* **2010**, 80, 381.
- [37] S. Kertit, B. Hammouti, *Appl. Surf. Sci.* **1996**, 93, 59.
- [38] H.M. Abd El-Lateef, *Corros. Sci.* **2015**, 92, 104.

-
- [39] L. Afia, R. Salghi, A. Zarrouk, H. Zarrok, O. Benali, B. Hammouti, S.S. Al-Deyab, A. Chakir, L. Bazzi, *Port. Electrochim. Acta*, **2012**, 30, 267.
- [40] S. Martinez, I. Stern, *Appl. Surf. Sci.* **2002**, 199, 83.
- [41] T. Szauer, A. Brand, *Electrochim. Acta*, **1981**, 26, 1219.
- [42] L. Herrag, B. Hammouti, S. Elkadiri, A. Aouniti, C. Jama, H. Vezin, F. Bentiss, *Corros. Sci.* **2010**, 52, 3042.
- [43] L. G. da Trindade, R. S. Goncalves, *Corros. Sci.* **2009**, 51, 1578.
- [44] A.K. Singh, M.A. Quraishi, *Corros. Sci.* **2011**, 53, 1288.
- [45] M. Lebrini, F. Robert, C. Roos, *Int. J. Electrochem. Sci.* **2011**, 6, 847.
- [46] M. Faustin, A. Maciuk, P. Salvin, C. Roos, M. Lebrini, *Corros. Sci.* **2015**, 92, 28.
- [47] M.A. Migahed, A.M. Abdul-Raheim, A.M. Atta, W. Brostow, *Mater. Chem. Phys.* **2010**, 121, 208.
- [48] P. Li, J.Y. Lin, K.L. Tan, J.Y. Lee, *Electrochim. Acta*, **1997**, 42, 605.
- [49] S.S. Abdel Rehim, O.A. Hazzazi, M.A. Amin, K.F. Khaled, *Corros. Sci.* **2008**, 50, 2258.